Computational Modeling of Single Cell Migration: The Leading Role of Extracellular Matrix Fibers Supporting Material

Daniela K. Schlüter, †* Ignacio Ramis-Conde, ‡ and Mark A.J. Chaplain, †

† Division of Mathematics, The University of Dundee, Dundee, Scotland; and

‡ Universidad de Castilla la Mancha, Department of Mathematics, Faculty of Education, Cuenca, Spain

Keywords: cell-matrix interaction, force-based modelling, mathematical modelling, matrix remodelling, cell traction forces, cancer

*Correspondence: dkschlueter@maths.dundee.ac.uk

Modeling the cell movement

Cell movement is governed by the total forces acting on an individual cell. By calculating all the forces acting on a cell and then applying Newton's Law of Motion (ignoring inertia terms cf. (1) (2)), we obtain an equation for the cell velocity. Hence, by integrating this equation we can then calculate the displacement of an individual cell over time. The system we are modeling consists of individual cells interacting with individual matrix fibres and so the forces on an individual cell consist of a drag force which is balanced by the overall force generated by an individual cell through contact with the matrix fibres and a term accounting for underlying "noise". Therefore the governing equation of motion has the general form:

$$\mathbf{F}_{drag} = \sum_{f} \mathbf{F}_{fj} + \mathbf{f}_j(t), \tag{S1}$$

where $\mathbf{F}_{fj}$ is the force generated by an individual cell through contact with an individual matrix fibre, with the sum taken over the fibres which are in contact with the cell, and $\mathbf{f}_j(t)$ is the term accounting for "noise". These terms are described in detail below.

We assume that as in *in vitro* set-ups, the layer of matrix fibers and the cells migrating on the matrix are embedded in a gel-like suspension. Thus the drag force that acts on the cell can be modelled using Stoke's Law cf. (3):

$$\mathbf{F}_{drag} = c\eta\mathbf{v}_j, \tag{S2}$$

where c is the shape factor which is $6\pi r$ with r being the radius of a spherical object, η is the fluid viscosity and $\mathbf{v_j}$ is the velocity of cell j. However, here it is important to remember that cells moving over a 2D substrate are not spherical whereas Stoke's law is defined for spherical objects. We therefore use a variation of Stoke's law for nonspherical objects as developed in (4) and (5) by assuming that the cell has a symmetric, almost hemispherical shape with flat extension around the periphery. With this we can simplify the variation down to changing only the shape factor to $c = 16.7 \times d$, where d is the radius of the frontal area circle and 16.7 is chosen to be in between the estimated factors for a hemispherical cup and a flat disk given in (5). In order to calculate the radius of the circle with the same area as the area of a slice of the cell perpendicular to its velocity, we need to know its height and width which have been measured for migrating MDCK cells by Schneider et al. (6). We therefore know that the fontal area of a migrating MDCK cell is approximately the area of half an ellipse with minor radius 2.6μm and major radius 15μm and thus $A_{\frac{1}{2}Ellipse} = \frac{1}{2}\pi \times 2.6\mu\text{m} \times 15\mu\text{m}$. Therefore the radius of the circle with the same area as the area of the biggest slice of the cell perpendicular to its velocity is $\left(\frac{1}{2} \times 2.6 \times 15\right)^{1/2}\mu$m for these measures. Or more general $\left(\frac{1}{2}ab\right)^{1/2}$ where a and b are the minor and major axes of the ellipse, respectively. This leads to the following shape factor

$$c = 16.7\left(\frac{1}{2}ab\right)^{1/2}, \tag{S3}$$

where a and b are the minor and major axes of the ellipse that is given by a thin slice of the cell at its highest point. For the fluid viscosity η we assume a value of 10^2 poise which is one order of magnitude lower than the viscosity of the three dimensional matrix used in (3). This reflects the fact that our cells are embedded within a gel rather than a 3D matrix which has many components that the cell interacts with which effectively increases the viscosity.

As mentioned above, other factors can influence the migration of cells. Even in an *in vitro* setting where no growth factors are added or chemical gradients set up, small fluctuations in concentrations or small impurities can occur that will have a slight influence on the cell's behaviour. Therefore we add a noise term $\mathbf{f}_j(t)$, which is uncorrelated and has zero mean, to our equation of motion.

We now describe our calculation of the force $\sum_f \mathbf{F}_{fj}$ generated by an individual cell through contact with the nearby matrix fibers. In order to migrate a cell needs to establish front-rear polarity and form focal contacts with the matrix. The process of focal complex formation and its stabilisation to a focal contact which enables the cell to obtain the traction needed to move along the fiber, takes place on the order of minutes (7). In the model we assume a time of 10 minutes for this process. In our single cell migration simulations this process only occurs at the very start when we set an unpolarised cell on the matrix. In simulations with two cells, a cell can lose it's polarity when it contacts another cell and cannot extend anymore protrusions in that direction (contact inhibition of locomotion). In this case the cell will have to reestablish its front-rear polarity. Once a cell is polarised, the extracellular matrix influences the cell's movement through contact guidance. Whether or not a cell contacts a fibre is determined by the distance of the cell centre to the fibre. If the distance is equal to or smaller than the cell radius then the fibre and the cell are considered to be in contact.

A cell can move along a fiber in two directions. We assume, as Dallon et al. in (8), that a cell contacting a fiber will chose the direction of the fiber that requires it to make the smallest change in direction. The same is done when a cell is in contact with more than one fiber. We again choose the orientation of each fiber that would require the smallest directional change from the cell. Then we make a projection of the cell's previous polarity axis onto each of these orientated fibers (see figure S1). Adding up the projections and normalising the resulting vector, gives the cell's new polarity axis, $\mathbf{p}_j^{new}(t)$ for cell j as:

$$\mathbf{p}_j^{new}(t) = \frac{1}{\|\mathbf{p}_j^{new}(t)\|} \sum_i \frac{\mathbf{p}_j^{old}(t).\mathbf{w}_i}{|\mathbf{w}_i|^2} \mathbf{w}_i \tag{S4}$$

where $\mathbf{w}_i$ is the direction of fiber i.

The projections onto the fiber directions weight the 'input stimuli' that the cell encounters so that more weight is given to fibers closely aligned with the cell's polarity axis. The reason for this procedure is that we assume a cell's movement to be biased towards moving in

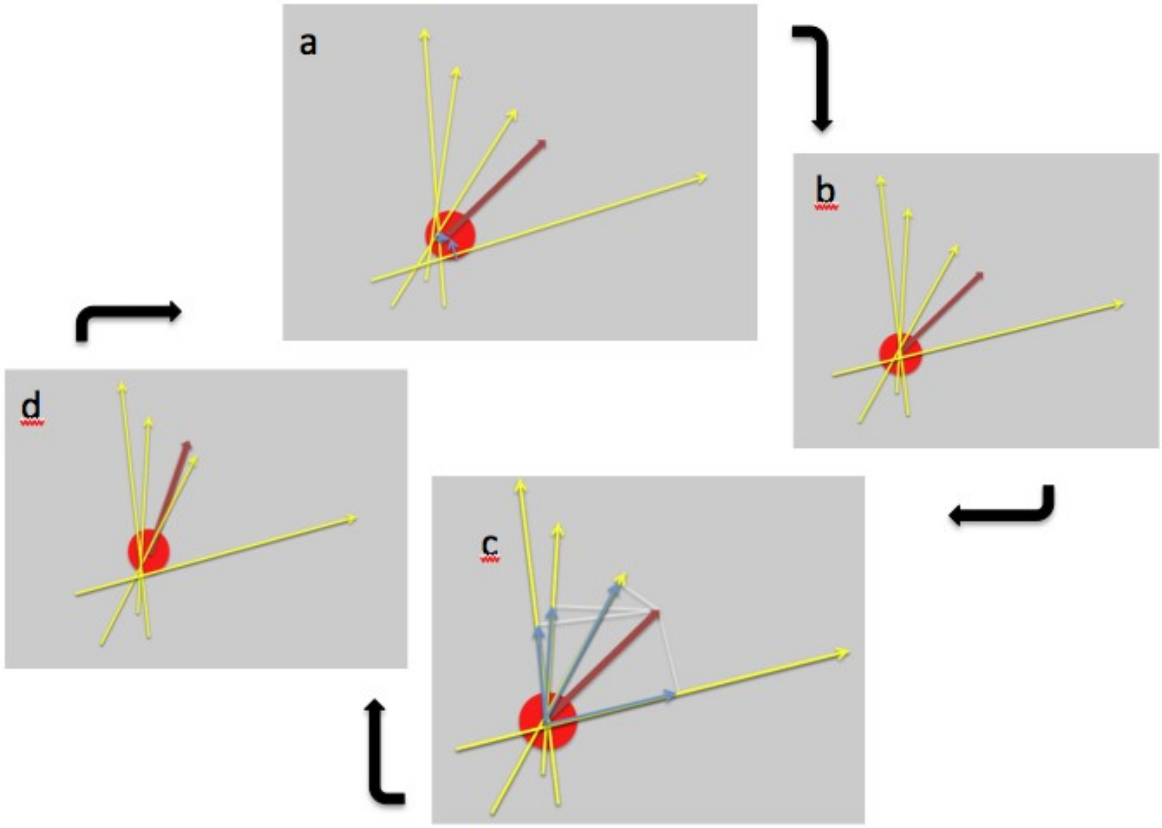

Figure S1: Schematic diagram showing the re-orientation of fibers by an individual cell and the subsequent calculation of the polarity axis and cell migration in this new direction.
(a) Re-orientation of the fibers by forces exerted by the cell (forces shown by blue arrows). (b) Choice of fiber orientation with the polarity axis of the cell being indicated by the dark red arrow. (c) Calculation of the new polarity axis by adding up the projections of the old polarity axis over all the fibers (blue arrows). (d) Movement of the cell along the new polarity axis according to the forces calculated.

the same direction it was moving in before, because all the integrins and other pro-migratory proteins are already clustered here. A change in direction would, in most cases, be due to a strong stimulus that causes the intracellular machinery to rearrange itself.

Note that equation (S4) gives a deterministic description of the cell's polarity axis. The stimulus that the cell encounters can however be stronger in one direction, not just due to the number of fibers, but also due to local fluctuations in the fibronectin and integrin distributions. We incorporate this by adding noise to the procedure explained above through the multiplication of the projection onto each fiber by $(1+\chi)$. χ is a Gaussian noise term with zero mean and a standard deviation of one. This gives a higher stochasticity to the influence of the fibers more closely aligned with the polarity axis than to those that are at a greater angle, i.e.

$$\mathbf{p}_j^{new}(t) = \frac{1}{\|\mathbf{p}_j^{new}(t)\|} \sum_i \frac{\mathbf{p}_j^{old}(t).\mathbf{w}_i}{|\mathbf{w}_i|^2} \mathbf{w}_i (1 + \chi_{ji}(t)) \tag{S5}$$

For cell j the net force generated through contact with the nearby matrix fibers is therefore given by:

$$\sum_f \mathbf{F}_{fj} = m\mathbf{p}_j^{new}(t) \tag{S6}$$

where m is the magnitude of the force, the calculation of which we now explain below.

We assume that for small time intervals ($t \in (t_i, t_i + \delta t)$), on average the cell maintains a uniform, straight movement following the direction determined by its interactions with nearby fibers. We model this by the use of a constant force term $\mathbf{K}$ derived from the contribution of each pseudopodia attached to a fibre i.e.

$$\sum_f \mathbf{F}_{fj} = \mathbf{K}_{t\in(t_i,t_i+\delta t)}. \tag{S7}$$

Hence, our equation of motion is now:

$$\mathbf{F}_{drag} = \mathbf{K}_{t\in(t_i,t_i+\delta t)} + \mathbf{f}_j(t). \tag{S8}$$

Since $\mathbf{f}_j(t)$ has zero mean, by taking the expected value we obtain that the force generated by a cell through interactions with the matrix fibers is proportional to the cell velocity:

$$\mathbf{F}_{drag} = c\eta\mathbf{v}_j = \mathbf{K}_{t\in(t_i,t_i+\delta t)}. \tag{S9}$$

The direction of the cell's movement is given by the polarity axis and thus we have that:

$$\mathbf{v}_j = speed \times \mathbf{p}_j^{new}(t). \tag{S10}$$

The direction of the net force is also along the polarity axis. Thus for $t \in (t_i, t_i + \delta t)$, we also have

$$\mathbf{K}_t = m\mathbf{p}_j^{new}(t). \tag{S11}$$

From equations (S9), (S10) and (S11) we see that the magnitude of the force, m, is proportional to the cell speed, i.e.

$$c\eta \times speed = m. \tag{S12}$$

Therefore we can use experimental measurements of the speed to calculate the magnitude of the force.

The speed at which a cell moves through extracellular matrix follows a biphasic behaviour and depends on integrin and ligand concentrations and the precise distribution of integrins over the cell surface (3, 9, 10). Apart from possible small local differences, we assume that

the ligand density is the same on all fibers and that 95 % of expressed integrins are at the front of the cell and therefore the speed is solely dependent on the integrin expression levels and the number of fibers a cell is in contact with. We further assume in all simulations an integrin expression level of 50% which leads to the maximum cell speed in respect to this parameter (10). In two dimensions the maximum speed a cell can reach on fibronectin is ≈ 20 μm/h which happens at approximately half the maximum adhesion force (10). In the simulations we however also investigate the effect of varying the value of this maximum cell speed. We assume the maximum cell-matrix adhesion is reached when a cell is in contact with 120 fibers as this would cover 80% of the cell-matrix contact area if the fibers were aligned.

Using this and the experimental measurements of cell speed dependent on adhesion force, we know how fast a cell should be moving given the number of fibers it is in contact with. Thus we calculate the magnitude m of the net force that a cell has to generate to pull itself forward at this speed from equation (S12). Plots in figure S2 show the relationship between number of fibres that a cell is in contact with and it's speed and the relationship between speed and the force.

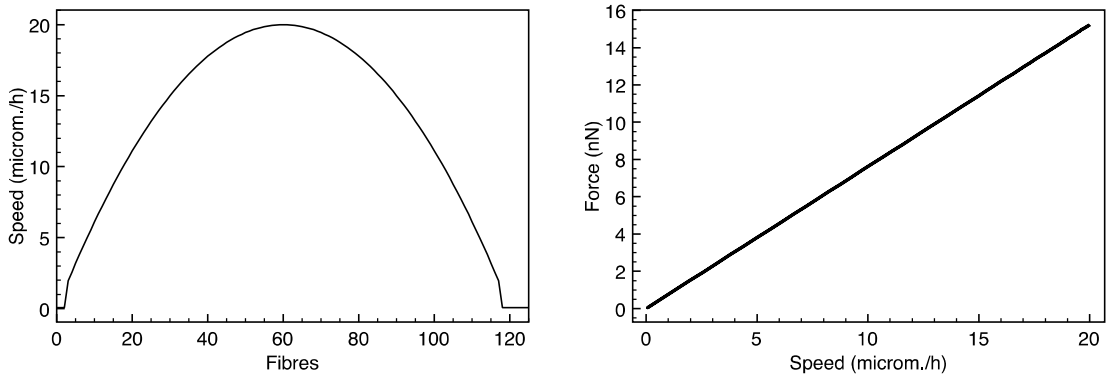

Figure S2: Plots showing the relationship between (a) the number of fibres a cells is in contact with and it's speed and (b) the speed and the force

Example of modeling the matrix rearrangement due to cell traction forces

The change in ϕ for different matrix stiffnesses can be seen in figure S3(a). In this figure we take the initial distance between the cell and the fiber (D) to be 15 μm which is the radius of the cell, the distance between the cell and the fulcrum (d) to be 50 μm (which gives a Θ value of 17.1887 degrees or 0.3047 radians) and the integrin expression (I) to be 0.5. The stiffness S varies between zero and one. We follow the development over 5 consecutive simulation time steps. The change of the angle between the fiber and the line connecting the fulcrum and the cell's centre (Θ) over these time steps can be seen in figure S3(b).

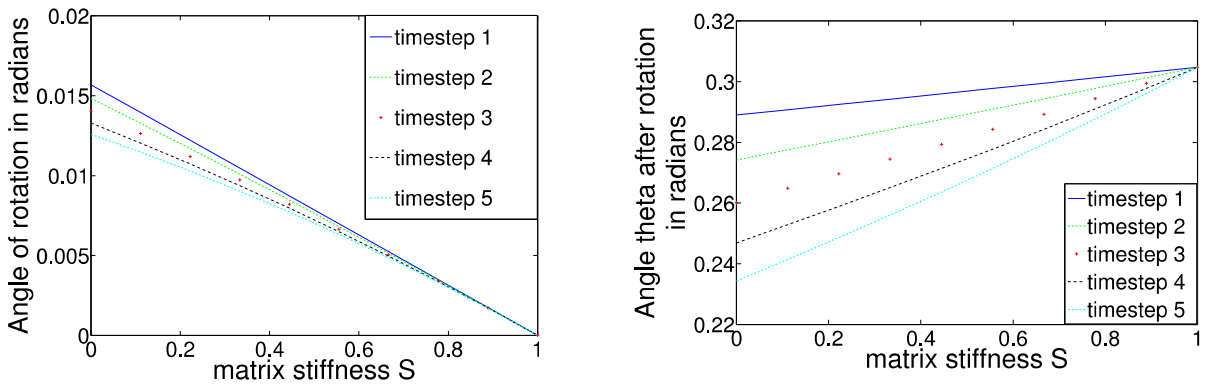

(a) (b)

Figure S3: Graphs showing the effects of matrix stiffness on the realignment of the fiber by equation (2) over five consecutive time steps.
(a) Graphs showing the angle of rotation ϕ depending on matrix stiffness (b) Graphs showing the angle between the straight line connecting the fulcrum and the cell's midpoint and the fiber (Θ) after the rotation.

Parameter values

The parameter values used in the computational simulations are presented in Table S1 along with the reference from where they were obtained.

parameter	value	reference
Radius of a cell base (R)	15μm	(6)
Height of a cell	2.6μm	(6)
Matrix fiber diameter	200nm	(11)
Suspension viscosity (η)	10^2 Poise	derived from (3)
Maximum cell speed in 2D	20μm/h	(10)
Focal complex formation time	10 min	(7)

Table S1: Table detailing the parameter values used in the computational simulations.

Software used in the data analysis and simulation

For the data analysis we calculate the persistence time by fitting our data to a persistent random walk model. The fit is done using the inbuilt MATLAB (MATLAB R2010a, The MathWorks, Natick, MA) function '*fminsearch*'. As outliers occurred for certain sets of simulations and the distribution of the results was very asymmetric, we used boxplots in these cases to visualise the data. They were done with R (version 2.13.1, The R Foundation for Statistical Computing). The model itself is implemented in C++. Fifteen simulations of one cell migrating on a matrix constituted of 15000 fibres over 3 days of real time takes approximately 10 hours of computational time on two 2.26GHz quadcore Intel Xeon processors.

Another external package was used for the generation of random numbers in the simulations. For this we used MERSENNE TWISTER random number generator (12).

The influence of matrix stiffness on persistence and migration speed

In figure S4 we present a more detailed study of the persistence time and mean actual speed of migration of an individual cell on matrices of varying stiffness S between 0.5 and 1. For these simulations we used the first matrix architecture considered in the main article. The plots in Fig.S4(a) and Fig.S4(b) show that both persistence time and mean speed are very similar between 0.5 and 0.9, but there appears to be some kind of transition between 0.9 and 1.

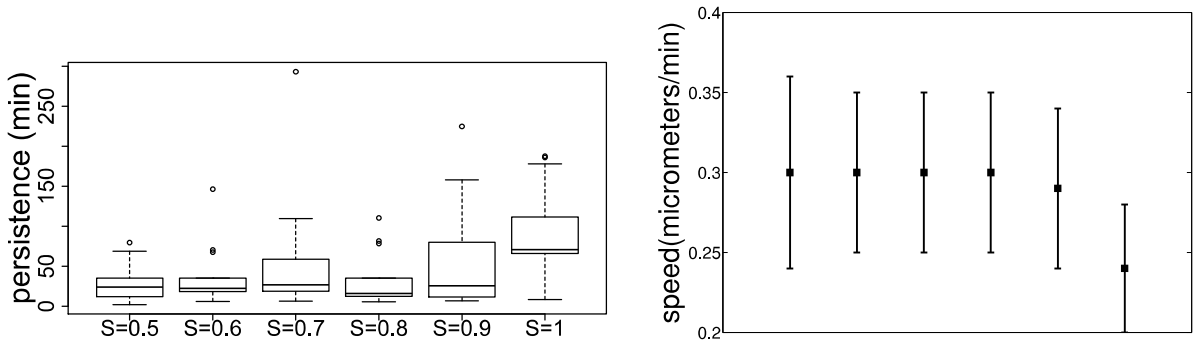

(a) (b)

Figure S4: Plots showing (a) the persistence time and (b) mean actual speed of migration of an individual cell on matrices of varying stiffness S between 0.5 and 1.

Sensitivity towards the noise term in the calculation of the polarity axis

One further element in the model might additionally influence the persistence of cells. This is the noise term χ that we add to the weight of each fiber in influencing the cell's direction of movement. In order to ensure that this does not have too big an impact on the results, we ran simulations with 25%, 50% and 100% increase and decrease of the standard deviation used to generate normally distributed numbers with zero mean. Again we ran 15 simulations for each value for the standard deviation and calculated the persistence time. The results are given in figure S5. In the simulations with standard deviations close to one, the persistent times are quite stable and no real impact of this parameter can be seen. If a bigger range is taken into account, it becomes obvious that an increase in standard deviation leads to a decrease in persistence although even here the difference is not very pronounced as the range of persistence times measured is very similar in all cases. Therefore it is clear that although this parameter has a slight influence on the results, it is by no means the determining factor.

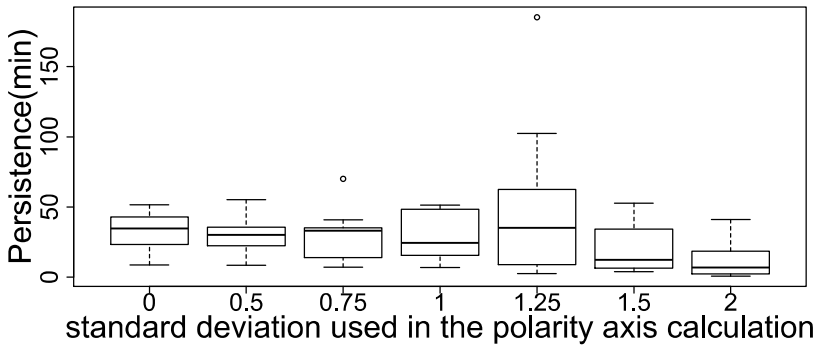

Figure S5: Plots showing the mean persistence time (in minutes) for different values of the standard deviations which were used to generate normally distributed numbers with zero mean for the noise term χ.

How does noise change a cell's behaviour?

Finally, we investigated the influence of the noise term $\mathbf{f}_j(t)$ on the cell's behaviour. For this we increased the standard deviation from 0 , which was used so far, to 0.0001, 0.001, 0.01, which was then of the same order of magnitude as the cell velocity per time step, and 0.1. Again we ran 15 simulations per standard deviation and the results for the persistence time can be seen in figure S6. For small standard deviations the influence of this noise term was minimal. Surprisingly the range in which the persistence times lie decreased for a standard deviation of 0.01. However as soon as the standard deviation became higher than the maximum cell speed per time step, the range of values for the persistence time became bigger which is what we would expect. Nonetheless, it is encouraging to see that for smaller standard deviations up to the order of magnitude of the cell velocity, the noise does not have a big effect on the results and the model is thus insensitive to small perturbations in this parameter as well as other parameters as we have seen above.

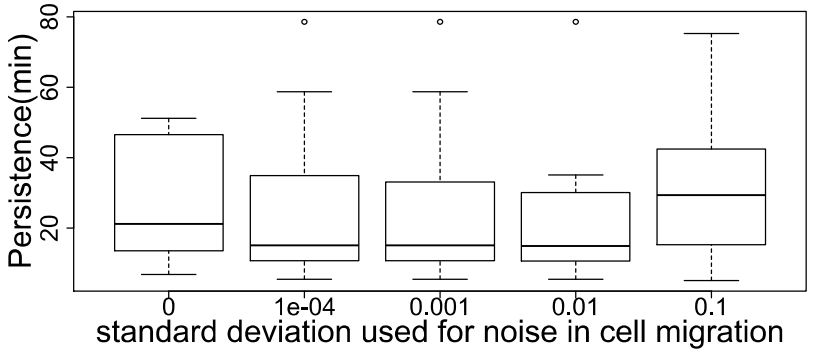

Figure S6: Plots of the persistence time (minutes) of cell migration where the standard deviation in the noise term $\mathbf{f}_j(t)$ is varied from 0 to 0.1.

Influence of parameters in modeling the matrix rearrangement due to cell traction forces

We investigated the influence of two parameters used in calculating the matrix rearrangement due to cell traction forces on the results of the simulations. The first parameter we looked at was the factor 0.1 which reduces the reorientation (Equation (2) of paper). The results of varying this parameter by 10% and 20% are shown in figure S7. It can be seen that the results are not very sensitive to this parameter as although the spread increases by varying it, the median changes very little.

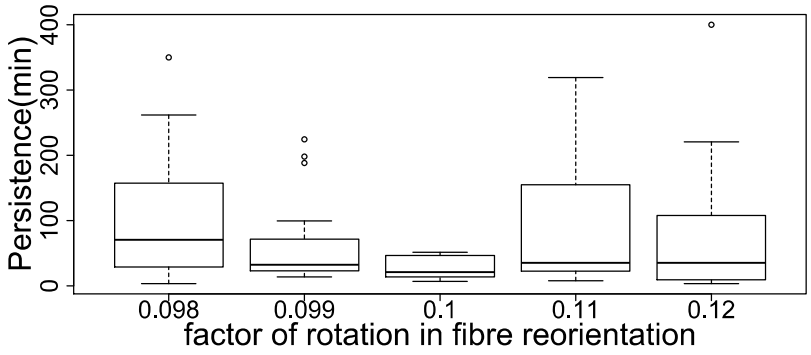

Figure S7: Plots of the persistence time (minutes) of cell migration where the factor that reduces the reorientation (given a value of 0.1 in equation (2)) is varied by 10% and 20%

The second parameter we investigated closer was the number of fibre cross-links at which we say the maximum stiffness of 0.95 is reached. Again we varied this number from it's initial value of 15 by 10% and 20%. The results are shown in figure S8. In this case the spread of the results increases again but similarly the median changes very little.

Modelling two cell migration: For how long do cells follow each other and what influences this behaviour?

On examining our computational simulation results, we noticed that two cells starting off close together or coming close to each other during the simulation time had a tendency to follow each other. In order to investigate this behaviour more thoroughly, we ran four different sets of simulations with 15 simulations per set. First we placed two cells very close together and kept one cell stationary for 10 minutes while the other could polarise and start migrating as was done in the simulation seen in figure 10. In the second set of simulations we started the two cells off far away from each other but again kept one of them stationary for the first 10 minutes. In the other two simulation setups we used a stiff, non-reorientable matrix. Again we ran one set with the cells starting off close together and one where they are initially placed far apart. For each set we ran 15 simulations in each of which we used a

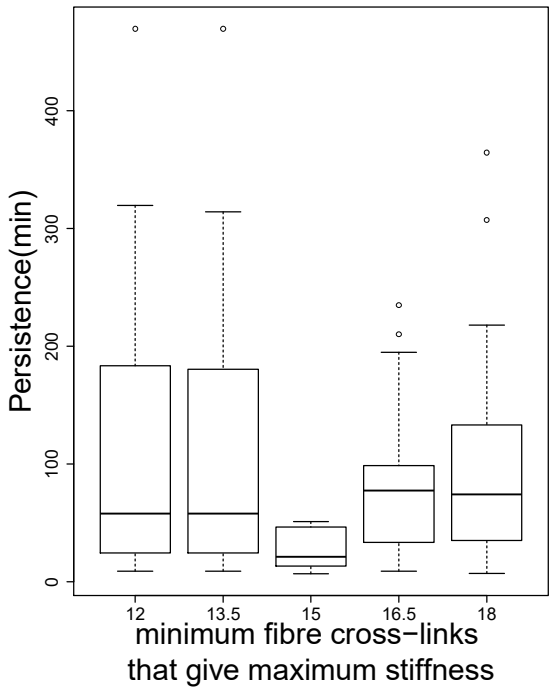

Figure S8: Plots of the persistence time (minutes) of cell migration where the number of fibre cross-links at which the maximum stiffness is reached is varied by 10% and 20% around the original value 15.

different seed for the random number generator used for the cell movement as was done in previous simulations. In order to determine whether or not cells were following each other, we calculated a distance matrix of each point on the first cell's track to each point on the other cell's track. Then we searched for all the time points where the cells were closer than two cell radii and tracked how long these episodes lasted for. We did these for all 15 simulations in each set and calculated the distribution of the length of time cells stayed closer than two cell radii. The results can be seen in figure S9. If the cells did not come close enough it was not counted at all, and therefore zeros in these plots denotes the cells just coming together at one point in time.

The plots in figure S9 clearly show that cells which start off close together on stiffer matrices follow each other for longer periods of time - figure S9(c) shows that cells can spend times of up to 1300 seconds close to each other (which is over 20 minutes), compared to 400-700 seconds in figures S9(a), (b), (d). If cells start far away from each other, the peak of the distribution is shifted to the right slightly so in most cases cells will follow each other for slightly longer periods of time. A reason for this may be that they do not encounter each other quite so quickly and lose their polarised state.

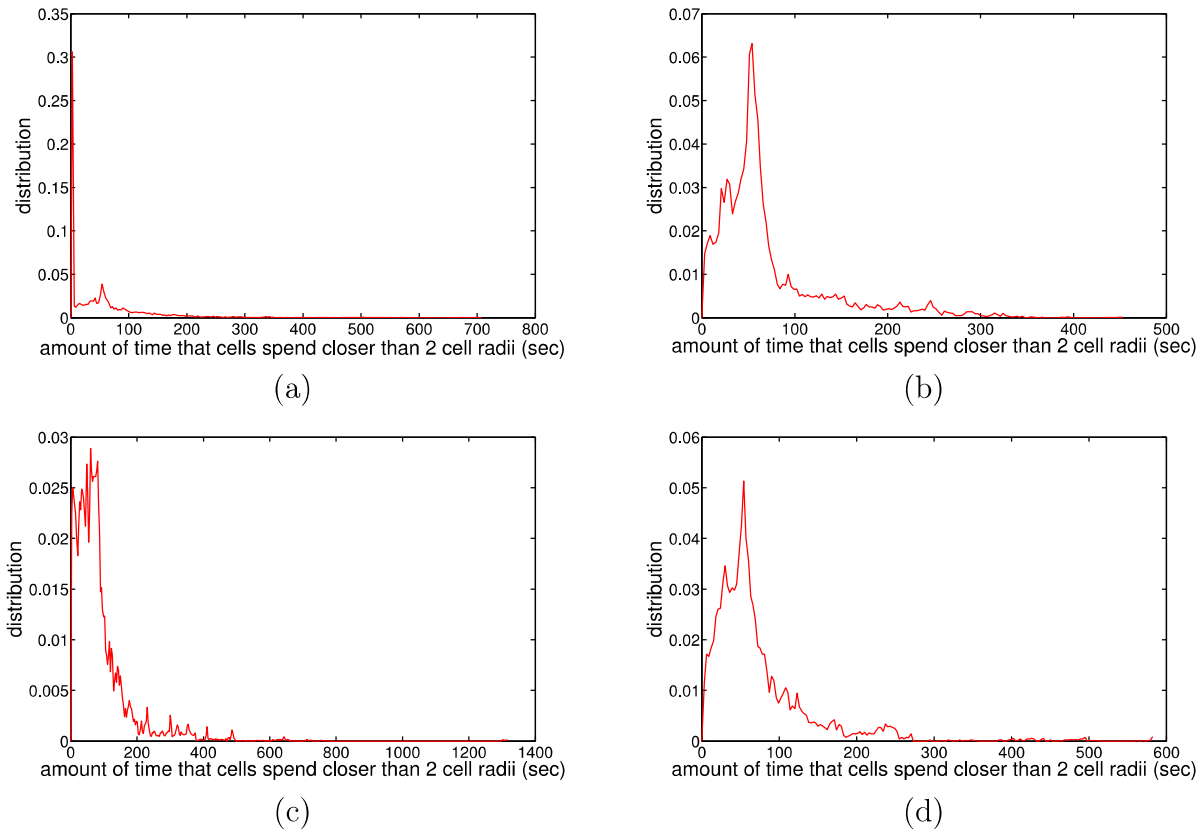

Figure S9: Plots showing the distribution of the amount of time that cells are closer than two cell radii. (a) Distribution of the time lengths for two cells starting close together and reorienting the matrix during movement. (b) Distribution of the time lengths for two cells starting far away from each other and reorienting the matrix during movement. (c) Distribution of the time lengths for two cells starting close together on a stiff, non-reorientable matrix. (d) Distribution of the time lengths for two cells starting far away from each other on a stiff, non- reorientable matrix.

Supporting References

[1] Galle, J., M. Loeffler, and D. Drasdo, 2005. Modeling the effect of deregulated proliferation and apoptosis on the growth dynamics of epithelial cell populations in vitro. *Biophys. J.* 88:62–75.

[2] Ramis-Conde, I., D. Drasdo, A. R. A. Anderson, and M. A. J. Chaplain, 2008. Modelling the influence of the E-cadherin-beta-catenin pathway in cancer cell invasion: A multiscale approach. *Biophys. J.* 95:155–165.

[3] Zaman, M. H., R. D. Kamm, P. Matsudaira, and D. A. Lauffenburger, 2005. Computational model for cell migration in three-dimensional matrices. *Biophys. J.* 89:1389–1397.

[4] Leith, D., 1987. Drag on nonspherical objects. *Aerosol Science and Technology* 6:153–161.

[5] Payne, L. E., and W. H. Pell, 1959. The Stokes flow problem for a class of axially symmetric bodies. *Fluid Mechanics* 7:529–549.

[6] Schneider, S. W., P. Pagel, C. Rotsch, T. Danker, H. Oberleither, M. Radmacher, and A. Schwab, 2000. Volume dynamics in migration epithelial cells measured with atomic force microscopy. *Eur J Physiol* 439:297–303.

[7] Friedl, P., and K. Wolf, 2003. Tumour-cell invasion and migration: Diversity and escape mechanisms. *Nature Reviews Cancer* 3:362–374.

[8] Dallon, J. C., J. A. Sherratt, and P. K. Maini, 1999. Mathematical modelling of extracellular matrix dynamics using discrete cells: Fibre orientation and tissue regeneration. *J. Theor. Biol.* 199:449–471.

[9] DiMilla, P. A., K. Barbee, and D. A. Lauffenburger, 1991. Mathematical model for the effects of adhesion and mechanics on cell migration speed. *Biophys. J.* 60:15–37.

[10] Palecek, S. P., J. C. Loftus, M. H. Ginsberg, D. A. Lauffenburger, and A. F. Horwitz, 1997. Integrin-ligand binding properties govern cell migration speed through cell-substratum adhesiveness. *Nature* 385:537–540.

[11] Friedl, P., K. Maaser, C. E. Klein, B. Niggemann, G. Krohne, and K. S. Zanker, 1997. Migration of highly aggressive MV3 Melanoma cells in 3-dimensional collagen lattices reults in local matrix reorganisation and shedding of $\alpha 2$ and $\beta 1$ integrins and CD44. *Cancer Res.* 57:2061–2070.

[12] Matsumoto, M., and T. Nishimura, 1998. Mersenne Twister: A 623-dimensionally equidistributed uniform pseudo-random number generator. *ACM Transactions on Modeling and Computer Simulation* 8:3–30.